NOAA'S HYSPLIT ATMOSPHERIC TRANSPORT AND DISPERSION MODELING SYSTEM

BY A. F. STEIN, R. R. DRAXLER, G. D. ROLPH, B. J. B. STUNDER, M. D. COHEN, AND F. NGAN

This work presents HYSPLIT's historical evolution over the last three decades along with recent model developments and applications.

The National Oceanic and Atmospheric Administration (NOAA) Air Resources Laboratory's (ARL) Hybrid Single-Particle Lagrangian Integrated Trajectory model (HYSPLIT) (Draxler and Hess 1998) is a complete system for computing simple air parcel trajectories as well as complex transport, dispersion, chemical transformation, and deposition simulations. HYSPLIT continues to be one of the most extensively used atmospheric transport and dispersion models in the atmospheric sciences community [e.g., more than 800 citations to Draxler and Hess (1998) on Web of Science; http://thomsonreuters.com/thomson-reuters-web-of-science/]. One of the most common model applications is a back-trajectory analysis to determine the origin of air masses and establish source–receptor relationships [Fleming et al. (2012) and references therein]. HYSPLIT has also been used in a variety of simulations describing the atmospheric transport, dispersion, and deposition of pollutants and hazardous materials. Some examples of the applications (Table 1) include tracking and forecasting the release of radioactive material (e.g., Connan et al. 2013; Bowyer et al. 2013; H. Jeong et al. 2013a), wildfire smoke (e.g., Rolph et al. 2009), wind-blown dust (e.g., Escudero et al. 2011; Gaiero et al. 2013), pollutants from various stationary and mobile emission sources (e.g., Chen et al. 2013), allergens (e.g., Efstathiou et al. 2011), and volcanic ash (e.g., Stunder et al. 2007).

The model calculation method is a hybrid between the Lagrangian approach, using a moving frame of reference for the advection and diffusion calculations as the trajectories or air parcels move from their initial location, and the Eulerian methodology, which uses a fixed three-dimensional grid as a frame of reference to compute pollutant air concentrations (the model name, no longer meant as an acronym, originally reflected this hybrid computational approach). The HYSPLIT model has evolved throughout more than 30 years, from estimating simplified single trajectories based on radiosonde observations to a system accounting for multiple interacting pollutants

AFFILIATIONS: STEIN, DRAXLER, ROLPH, STUNDER, AND COHEN—NOAA/Air Resources Laboratory, College Park, Maryland; NGAN—NOAA/Air Resources Laboratory, and Cooperative Institute for Climate and Satellites, College Park, Maryland
CORRESPONDING AUTHOR: Ariel F. Stein, NOAA/Air Resources Laboratory, R/ARL–NCWCP–Room 4205, 5830 University Research Court, College Park, MD 20740
E-mail: ariel.stein@noaa.gov

The abstract for this article can be found in this issue, following the table of contents.
DOI:10.1175/BAMS-D-14-00110.1

A supplement to this article is available online (10.1175/BAMS-D-14-00110.2)

In final form 27 April 2015

Table 1. Examples of studies using HYSPLIT for transport and dispersion calculations.

Application	Location	Brief description	Reference(s)
Radionuclides	Marshall Islands (central Pacific), Nevada Test Site (United States), Semipalatinsk Nuclear Test Site (Kazakhstan)	Deposition of fallout from atmospheric nuclear tests	Moroz et al. (2010)
	AREVA NC La Hague nuclear processing plant (northwestern France)	Krypton-85 air concentrations	Connan et al. (2013)
	Fukushima and adjacent prefectures (Japan)	Air parcel transport and dispersion to interpret iodine, tellurium, and cesium measurements	Kinoshita et al. (2011)
	80-km range around Fukushima reactor (Japan)	Temporal behavior of plume trajectory, concentration, deposition, and radiation dosage of cesium-137	Challa et al. (2012)
	Global	Transport, dispersion, and deposition of xenon-133	Bowyer et al. (2013)
	Metropolitan area of Seoul, South Korea	Radiological risk assessment due to radiological dispersion devices (RDDs) terrorism containing cesium-137	H. Jeong et al. (2013)
	Fukushima (Japan) and global	Emissions, transport, dispersion, deposition, and dosage of cesium-137 iodine-131	Draxler and Rolph (2012); Draxler et al. (2013)
	Nevada Test Site	Dispersion from nuclear test	Rolph et al. (2014)
Wildfire smoke	CONUS	U.S. National Weather Service Smoke Forecasting System	Rolph et al. (2009)
	CONUS	Sensitivity study to plume injection height	Stein et al. (2009)
Wind-blown dust	Northern Africa and Spain	Source attribution of dust originated from the Saharan Desert	Escudero et al. (2006, 2011)
	Australia	Forecast dust event of 22–24 Oct 2002	Wain et al. (2006)
	Saudi Arabia, Iraq, Syria, Jordan, and Iran	Emissions, transport, dispersion, and deposition of dust over Iran	Ashrafi et al. (2014)
	Northern Africa and southern Spain	Forecast dust for 2008 and 2009	Stein et al. (2011)
	Global	Two dust emission schemes and GEM used to simulate the global dust distribution for 2008	Wang et al. (2011)
	Patagonia (Argentina) and sub-Antarctic Atlantic Ocean	Dust event reaching Antarctica	Gasso and Stein (2007)

Table 1. Continued.			
Application	**Location**	**Brief description**	**Reference(s)**
	Puna–Altiplano deserts (Bolivia) and southern South America	Estimation of transport, dispersion, and deposition and comparison with satellite data	Gaiero et al. (2013)
Air pollutants	Mississippi Gulf Coast region (United States)	Mesoscale transport of air pollutants from point sources/sulfur dioxide and nitrogen oxides simulation	Challa et al. (2008)/ Yerramilli et al. (2012)
	Great Lakes (United States)	Transport and deposition of mercury and dioxins	Cohen et al. (2002, 2004, 2011, 2013)
	Houston, Texas (United States)	Transport and dispersion of benzene	Stein et al. (2007)
	Huelva (Spain)	Transport and dispersion of arsenic in particulate matter	Chen et al. (2013)
Allergens	Eastern United States	Emission and transport of pollen	Efstathiou et al. (2011)
	Central Northern United States	Emission and transport of pollen	Pasken and Pietrowicz (2005)
Volcanic ash	North America	Forecast ash transport	Stunder et al. (2007)

transported, dispersed, and deposited over local to global scales. In this paper we walk the reader through the model's history describing the ideas that inspired its inception, the evolution of the scientific concepts and parameterizations that were incorporated into successive model versions, and the most recent innovations.

MODEL HISTORICAL BACKGROUND: 1940s–70s.

The scientific foundation and inspiration for HYSPLIT's trajectory capabilities can be traced back to 1949 (Fig. 1), when the Special Project Section (SPS) (ARL's predecessor) of the U.S. Weather Bureau [now NOAA's National Weather Service (NWS)] was charged with trying to find the source of radioactive debris originating from the first Soviet atomic test and detected by a reconnaissance aircraft near the Kamchatka Peninsula. For that purpose, back trajectories were calculated by hand based on wind data derived from twice-daily radiosonde balloon measurements. These trajectories followed 500-hPa heights assuming geostrophic wind flow. Although these back trajectories were calculated more than 60 years ago, the percentage error between the calculated and actual source location relative to the distance covered by the trajectories was remarkably low (about 5%; Machta 1992). Since then, trajectory calculations have been one of the backbones of ARL's research activities (e.g., Angell et al. 1966, 1972, 1976).

During the mid-1960s, Pasquill (1961) and Gifford (1961) described the estimation of the horizontal and vertical standard deviation of a continuous plume concentration distribution, which constituted the basis for the construction of the so-called Gaussian dispersion models. One such model was developed at ARL (Slade 1966, 1968; Fig. 1) based on data from the well-known Project Prairie Grass (Barad 1958). Using this Gaussian approach and assuming steady state with homogeneous and stationary turbulence, air concentrations were estimated based on wind data collected at a single site. Extending this work in the late 1960s and early 1970s to handle more realistic (changing) weather conditions, ARL scientists developed the Mesoscale Diffusion (MESODIFF) model (Start and Wendell 1974; Fig. 1) in response to health and safety concerns at the Idaho National Reactor Testing Station (NRTS) related to planned or accidental releases of radioactive material into the atmosphere. This segmented Gaussian puff model used gridded data interpolated from a network of 21 tower-mounted wind sensors located within the boundaries of the NRTS (Wendell 1972) to account for spatial variability of the horizontal wind flow near the surface. The simulations used a maximum of 400

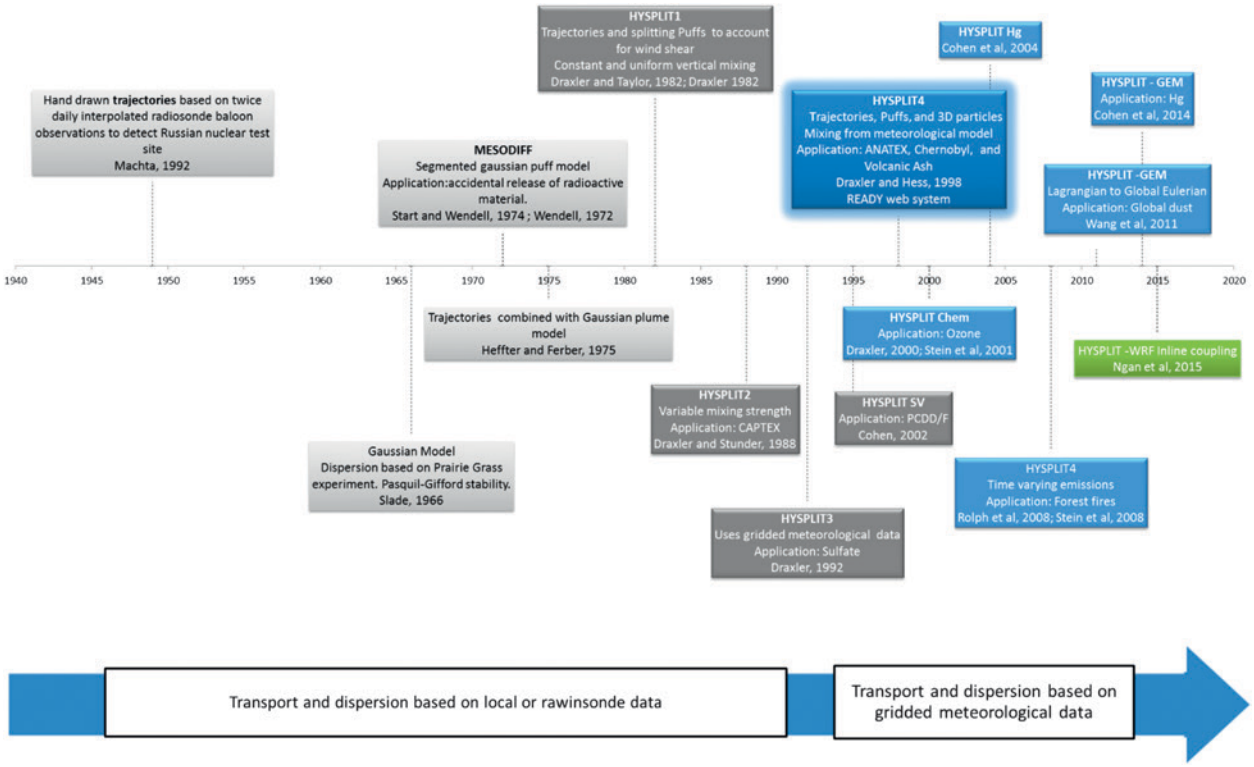

Fig. 1. History of the HYSPLIT model. The light gray shade describes models that influenced HYSPLIT. The dark gray shade corresponds to the first three versions of the HYSPLIT system. The dark blue box corresponds to HYSPLIT4 and the light blue boxes correspond to applications that derive from HYSPLIT4.

puffs and incorporated time-varying diffusion rates. A similar approach was used during the mid-1970s, when ARL researchers (Heffter et al. 1975) combined trajectories with a Gaussian plume model to compute long-range air concentrations from gaseous or particulate emissions from a uniform, continuous point source based on rawinsonde data.

HYSPLIT DEVELOPMENT HISTORY: 1980s–2000s. These previous dispersion studies established the scientific basis for the development of HYSPLIT, version 1 (HYSPLIT1), in the early 1980s (Draxler and Taylor 1982; Fig. 1). In this initial version, segmented pollutant puffs were released near the surface and their trajectories were followed for several days. Transport was calculated from wind observations based on rawinsonde data (not interpolated) taken twice daily. Assumptions included no vertical mixing at night and complete mixing over the planetary boundary layer (PBL) during the day. Nocturnal wind shear was modeled by vertically splitting the puffs that extended throughout the PBL into 300-m subpuffs during the nighttime transport phase of the calculation. The model was used to simulate Kr-85 released to the atmosphere and sampled at multiple locations in the Midwestern United States during a 2-month field experiment (Draxler 1982). Later on, HYSPLIT version 2 (HYSPLIT2; Fig. 1) included the use of interpolated rawinsonde or any other available measured data to estimate vertical mixing coefficients that varied in space and time (Draxler and Stunder 1988). These mixing coefficients were derived from the Monin–Obukhov length, friction velocity, and surface friction potential temperature (Draxler 1987). This model version was applied to simulate the Cross Appalachian Tracer Experiment (CAPTEX; Ferber et al. 1986). Before the early 1990s, HYSPLIT only used rawinsonde observations with very limited spatial (e.g., 400 km) and temporal (e.g., 12 h) resolution for the calculation of transport and dispersion. Not until development of HYSPLIT version 3 (HYSPLIT3; Fig. 1) did the model utilize gridded output from meteorological models such as the Nested Grid Model (NGM; Table 2). HYSPLIT3 allowed the calculation of trajectories as well as transport and dispersion of pollutants using cylindrical puffs that grow in time and split when reaching the grid size of the meteorological data (Draxler 1992). This version was applied to simulate the Across North America Tracer Experiment (ANATEX; Draxler and

Table 2. Publicly available analysis meteorological data files to run HYSPLIT.

Model	Horizontal resolution	Time period available	Output frequency	Geographical coverage	Reference(s)
NCEP/GDAS	1°	Dec 2004–present	3 h	Global	Kanamitsu (1989)
NCEP/GDAS	0.5°	Sep 2007–present	3 h	Global	Kanamitsu (1989)
NCEP–NCAR reanalysis	2.5°	1948–present	6 h	Global	Kalnay et al. (1996)
NCEP/North American Mesoscale (NAM)	12 km	Jun 2007–present	3 h	CONUS	Black (1994); Janjić (2003); Janjić et al. (2005)
NCEP/Eta forecast model analysis fields [the Eta Data and Assimilation System (EDAS)]	40 km	2004–present	3 h	CONUS	Black (1994)
NCEP/Eta forecast model analysis fields (EDAS)	80 km	1997–2004	3 h	CONUS	Black (1994)
NCEP/Nested Grid Model (NGM)	180 km	Jan 1991–Apr 1997	2 h	CONUS	Philips (1979); Hoke et al. (1989)
NCEP/North American Regional Reanalysis (NARR)	32 km	1979–present	3 h	CONUS	Mesinger et al. (2006)

Heffter 1989). Chemical formation and deposition of sulfate (SO^4_{2-}; Rolph et al. 1992, 1993a) were incorporated into HYSPLIT3 in a first attempt to include chemistry in the modeling system. This application incorporated gas- and aqueous-phase oxidation of sulfur dioxide (SO_2) and dry and wet removal of SO_2 and aerosol SO^4_{2-}. In HYSPLIT3, chemical transformations occurred only within each Lagrangian puff, without any interaction with other puffs. As part of a broader acid precipitation research effort, the model was applied over the eastern United States for 1989 and compared against observed seasonal and annual spatial patterns of SO_2 and SO^4_{2-} concentrations in air and wet deposition of SO^4_{2-} from precipitation. HYSPLIT3 was also used to model the atmospheric fate and transport of semivolatile (SV) pollutants by incorporating a dynamic vapor/particle partitioning algorithm and including chemical transformations initiated by the hydroxyl radical (OH) and photolysis. HYSPLIT-SV has been used to estimate the transport and deposition of polychlorinated dibenzo-p-dioxin and polychlorinated dibenzofurans (PCDD/F) to the Great Lakes, including the estimation of detailed source–receptor relationships (Cohen et al. 1995, 1997b, 2002). Also, HYSPLIT-SV was utilized to obtain source–receptor results for atrazine transport and deposition to the Great Lakes and other sensitive ecosystems (Cohen et al. 1997a).

By the end of the 1990s, many new features had been incorporated into HYSPLIT version 4

(HYSPLIT4; Draxler and Hess 1998; Fig. 1), the basis for current model versions. The innovations include an automated method of sequentially using multiple meteorological grids going from finer to coarser horizontal resolution (e.g., Table 2) and the calculation of the dispersion rate from the vertical diffusivity profile, wind shear, and horizontal deformation of the wind field. HYSPLIT4 allows the use of different kinds of Lagrangian representations of the transported air masses: three-dimensional (3D) particles, puffs, or a hybrid of both. A 3D "particle" is a point, computational mass—representing a gaseous or particulate-phase pollutant—moved by the wind field with a mean and a random component (see section on "Transport, dispersion, and deposition calculation" and the online supplement, which can be found online at http://dx.doi.org/10.1175/BAMS-D-14-00110.2). Individual 3D particles never grow or split, but a sufficient number needs to be released to represent the downwind horizontal and vertical pollutant distribution. A single puff, on the other hand, represents the distribution of a large number of 3D particles by assuming a predefined concentration distribution (Gaussian or top hat) in the vertical and horizontal directions. They grow horizontally and vertically according to the dispersion algorithms for puffs [see Draxler and Hess (1998) for details], equivalent to the evolving distribution of particles in a comparable 3D particle calculation. Furthermore, puffs split if they become too large to be represented by a single meteorological data point. To avoid the puff number quickly reaching the computational array limits, puffs of the same age occupying the same location may be merged (see online supplement for details about splitting and merging). An alternative approach is to simulate the dispersion with a 2D object (planar mass, having zero vertical depth), where the contaminant has a puff distribution in the horizontal direction, growing according to the dispersion rules for puffs and splitting if it gets too large. In the vertical, however, they are treated as Lagrangian particles. This option permits the model to represent the more complex vertical structure of the atmosphere with the higher fidelity possible when using particles while representing the more uniform horizontal structure using puffs.

Version 4 of HYSPLIT has been the basis for the construction of essentially all model applications for the last 15 years. It has been evaluated against ANATEX observations and has been applied to estimate radiological deposition from the Chernobyl accident (Kinser 2001) and to simulate the Rabaul volcanic eruption (Draxler and Hess 1997, 1998). At the beginning of the 2000s, applications started to incorporate nonlinear chemical transformation modules to simulate ozone (O_3) in the lower troposphere. Specific examples are given below, but in general, incorporating nonlinear chemical processes into a Lagrangian framework such as HYSPLIT constitutes a challenging task because there is no simple approach to deal with the chemical interactions that can occur among Lagrangian particles or puffs. The usual approach is to rely on a Lagrangian methodology to compute transport, dispersion, and deposition and an Eulerian framework to represent the chemical transformations of different reactive species (Chock and Winkler 1994b).

Draxler (2000) included a simplified photochemical scheme that describes the formation of tropospheric O_3 using the integrated empirical rate (IER) chemical module (Johnson 1984; Azzi et al. 1995). The model configuration was very similar to that of Rolph et al. (1992), using a Lagrangian approach to simulate the transport, dispersion, and deposition and an Eulerian framework to calculate the O_3 concentrations with no interaction among puffs. Using HYSPLIT driven by the Eta Data Assimilation System (EDAS) meteorological dataset (Table 2), this approach was applied to the area of Houston, Texas, for the summer of 1997.

A more generalized nonlinear chemistry module was incorporated into HYSPLIT (HYSPLIT CheM) to calculate the spatial and temporal distribution of different photochemical species in the lower troposphere over a regional scale (Stein et al. 2000). Using 3D particles, transport and dispersion were computed using meteorological fields from a mesoscale model [e.g., fifth-generation Pennsylvania State University–National Center for Atmospheric Research Mesoscale Model (MM5)]. Once the concentrations of all the chemicals were calculated over a regular Eulerian grid by summing the masses of the particles in the box where they reside, the Carbon Bond IV (Gery et al. 1989) mechanism was used to model chemical transformations. The resulting concentrations from the chemical evolution of each species were then redistributed as a change in the mass of each particle within the cell. It was assumed that the ratio of the final to initial concentration is equal to the ratio of the final to the initial mass for the corresponding species (Chock and Winkler 1994b; Stein et al. 2000). HYSPLIT CheM was applied to simulate O_3 concentrations in Pennsylvania for a case study in 1996 (Stein et al. 2000). In addition, this particular model application constituted the first routine implementation of the particle-in-grid approach applied to the forecast of air quality (Kang et al. 2005).

At about the same time, HYSPLIT-SV was updated to the HYSPLIT4 framework and was used to estimate the transport and deposition of PCDD/F to the Great Lakes (Cohen et al. 2002) and to later estimate the fate and transport of PCDD/F emitted from the in situ burning of sea surface oil following the Deepwater Horizon spill (Schaum et al. 2010). In addition, HYSPLIT-SV was extended to simulate atmospheric mercury (HYSPLIT-Hg) by adding new gas-phase reactions and a treatment of aqueous-phase equilibrium and chemistry. Spatiotemporally resolved reactant concentrations (e.g., O_3, OH, SO_2) were estimated for each puff based on external model results and/or algorithms based on empirical data. This puff-based version of HYSPLIT-Hg has been used to analyze the transport and deposition of mercury to the Great Lakes from U.S. and Canadian sources (Cohen et al. 2004) and the fate and transport of mercury emissions in Europe (Ryaboshapko et al. 2007a,b).

By the end of the 2000s, new emissions features were included that are more sophisticated than the explicit input of an emission rate—that is, how much mass is assigned to each particle. Two predefined emission algorithms result in time-varying emissions based upon changing meteorological conditions. The first application for this approach, for wind-blown dust, relied on the calculated friction velocity and satellite-derived land use information to estimate the emissions. This algorithm (see online supplement) was applied to estimate dust levels over the contiguous United States (Draxler et al. 2010) and globally (Wang et al. 2011). The second time-varying emission algorithm allows for the estimation of plume rise using the buoyancy terms based on heat release, wind velocity, and friction velocity. This parameterization (online supplement) has been applied to predict transport and dispersion of smoke originating from forest fires over the contiguous United States (Rolph et al. 2009; Stein et al. 2009), Alaska, and Hawaii, and was used in the simulation of emissions from in situ sea surface oil burning (Schaum et al. 2010).

RECENT MODEL DEVELOPMENTS. *Transport, dispersion, and deposition calculation.* Many upgrades that reflect the most recent advances in the computation of dispersion and transport have been incorporated into HYSPLIT over the last 15 years. Only a brief introduction is given here; further details can be found in the online supplement. The computation of the new position at a time step ($t + \Delta t$) due to the mean advection by the wind determines the trajectory that a particle or puff will follow. In other words, the change in the position vector $\mathbf{P}_{\text{mean}}$ with time

$$\mathbf{P}_{\text{mean}}(t+\Delta t) = \mathbf{P}_{\text{mean}}(t) + \frac{1}{2}\Big[\mathbf{V}(\mathbf{P}_{\text{mean}}, t) + \mathbf{V}\Big(\Big\{\mathbf{P}_{\text{mean}}(t) + \big[\mathbf{V}(\mathbf{P}_{\text{mean}}, t)\Delta t\big]\Big\}, t+\Delta t\Big)\Big]\Delta t \quad (1)$$

is computed from the average of the three-dimensional velocity vectors $\mathbf{V}$ at their initial and first-guess positions (Draxler and Hess 1998). Equation (1) is the basis for the calculation of trajectories in HYSPLIT. Only the advection component is considered when running trajectories. The turbulent dispersion component is only needed to describe the atmospheric transport and mixing processes for 3D particles and puffs.

The dispersion equations are formulated in terms of the turbulent velocity components. In the 3D particle implementation of the model, the dispersion process is represented by adding a turbulent component to the mean velocity obtained from the meteorological data (Fay et al. 1995); namely,

$$X_{\text{final}}(t+\Delta t) = X_{\text{mean}}(t+\Delta t) + U'(t+\Delta t)\Delta t \quad \text{and} \quad (2)$$

$$Z_{\text{final}}(t+\Delta t) = Z_{\text{mean}}(t+\Delta t) + W'(t+\Delta t)\Delta t, \quad (3)$$

where U' and W' correspond to the turbulent velocity components, X_{mean} and Z_{mean} are the mean components of particle positions, and X_{final} and Z_{final} are the final positions in the horizontal and vertical, respectively. The turbulence component is always added after the advection computation.

Here, U' and W' are calculated based on the modified discrete-time Langevin equation [Chock and Winkler (1994a) and references therein], which is expressed as a function of the velocity variance, a statistical quantity derived from the meteorological data, and the Lagrangian time scale. Four updated model parameterizations are available for the calculation of vertical mixing—namely, i) assuming the vertical mixing diffusivities follow the coefficients for heat, ii) based on the horizontal and vertical friction velocities and the PBL height, iii) using the turbulent kinetic energy (TKE) fields, or iv) directly provided by the meteorological data. Furthermore, a very simplified enhanced mixing deep convection parameterization based on the convective available potential energy has been included (see the online supplement).

The description of how wet and dry deposition is simulated in HYSPLIT can be found elsewhere (Draxler and Hess 1998). However, a new option for in-cloud wet scavenging parameterization has been incorporated

into the modeling system based on the estimation of a scavenging coefficient (Leadbetter et al. 2015; see the online supplement for further details).

Embedded global Eulerian model (GEM) and multiple Lagrangian representations. Recently, a global Eulerian model (GEM; Draxler 2007) was included as a module of the HYSPLIT modeling system. In this option, particles or puffs are first released in the Lagrangian framework and carried within HYSPLIT until they exceed a certain age at which point their mass is transferred to the GEM. Currently, the GEM can only be driven by global meteorological data from the Global Forecast System (GFS), Global Data Assimilation System (GDAS), or the National Centers for Environmental Prediction (NCEP)–National Center for Atmospheric Research (NCAR) reanalysis models (Table 2). The GEM includes the following processes: advection, horizontal and vertical mixing, dry and wet deposition, and radioactive decay. One advantage of this approach is that near the emission sources the Lagrangian calculation better depicts the details of the plume structure, without the initial artificial diffusion of an Eulerian model. Then, when the plume features no longer need to be resolved, the particle or puff mass is transferred to the Eulerian framework. The GEM calculation methodology is primarily aimed at improving the computational efficiency of global transport applications and especially in situations when shorter-range plumes may interact with hemispheric or global background variations. In such cases, a single simulation can be used to efficiently model global transport, dispersion, and deposition that would be computationally burdensome using 3D particles or puffs alone considering the number of such particles or puffs that would be required for global coverage. In particular, this approach is very effective in simulating the initiation of individual dust storm plumes that quickly merge into a regional or even hemispheric event (e.g., Wang et al. 2011). In addition, the mercury analysis performed to estimate North American sources influencing the Great Lakes area has recently been extended using the GEM capability within HYSPLIT to include sources worldwide (Cohen et al. 2011, 2014).

Besides transferring the mass from puff/particles to the GEM, HYSPLIT recently incorporated an option to allow the Lagrangian description to change between particles and puffs during the transport process depending upon their age (since release); this is called the mixed-mode approach. This option attempts to avoid dealing with a large number of particles while keeping the best physical description of the phenomenon under study. For instance, a mixed mode may be selected to take advantage of the more accurate representation of the 3D particle approach near the source and the horizontal distribution information provided by one of the hybrid puff approaches at longer transport distances. The following transformation options are available in the HYSPLIT system: 3D particle converting to Gaussian horizontal puff and vertical particle distribution (Gh-Pv), 3D particle converting to top-hat horizontal puff and vertical particle distribution (THh-Pv), Gh-Pv converting to 3D particle, THh-Pv converting to 3D particle, and 3D particle or puffs (Gaussian or top hat) converting to the GEM. In general, fewer Lagrangian particles/puffs are needed under the mixed-mode approach for a given level of computational resolution.

Source estimations using footprints. Back-trajectory calculations have been one of the most attractive and prominent features by which HYSPLIT has been used in many studies [Fleming et al. (2012) and references therein]. Although trajectories offer a simple assessment of source–receptor relationships, a single trajectory cannot adequately represent the turbulent mixing processes that air parcels experience during transport. However, coupling the back-trajectory calculation with a Lagrangian dispersion component can produce a more realistic depiction of the link between the concentrations at the receptor and the sources influencing it (Stohl et al. 2002; Lin et al. 2003). To this end, backward-in-time advection with dispersion has been included in the HYSPLIT modeling system by simply applying the dispersion equations to the upwind trajectory calculation [i.e., Eqs. (2) and (3) are assumed to be reversible when integrated from $t + \Delta t$ to t]. Under this approach, the increasingly wider distribution of Lagrangian particles or puffs released from a receptor undergoing backward-in-time transport and dispersion represents the geographical extent and strength of potential sources influencing the location of interest. Nevertheless, this particular model application must satisfy the well-mixed criteria, include appropriate representation of the interaction between the wind shear and vertical turbulence, and provide for sufficient decay in the autocorrelation of U' [see Lin et al. (2003) for details]. In addition, the mean trajectory component of the calculation, which is normally considered to be reversible, should not intersect the ground; otherwise it loses information and becomes irreversible. From the practical computational perspective, performing backward calculations from a few receptor points is more efficient than forward calculations from many

more potential source locations to find the best match with the receptor data even at the loss of some accuracy. The more accurate forward calculation can be used once a smaller set of source locations have been identified.

Examples of the use of HYSPLIT's backward Lagrangian dispersion modeling methodology include the estimation of mercury sources impacting New York State (Han et al. 2005), backtracking anthropogenic radionuclides using a multimodel ensemble (Becker et al. 2007), and quantifying the origins of carbon monoxide and ozone over Hong Kong (Ding et al. 2013). In addition, this approach has been adopted in other applications that have used HYSPLIT as the foundational model for back dispersion calculations [e.g., the Stochastic Time-Inverted Lagrangian Transport (STILT) model: Lin et al. 2003; Wen et al. 2012]. Building upon this capability, HYSPLIT also allows for the direct calculation of source footprints (Lin et al. 2003), defined as areas of surface emission fluxes that contribute to changes in concentrations at a receptor (online supplement). Examples of the use of this approach can be found elsewhere (e.g., Gerbig et al. 2003; Kort et al. 2008; Zhao et al. 2009; S. Jeong et al. 2013).

Pre- and postprocessors. The preparation of the required meteorological input data and the analysis of the simulation outputs are important additional aspects to consider when running the HYSPLIT model. HYSPLIT includes a series of preprocessors designed to prepare model-ready meteorological gridded datasets and postprocessors to analyze multiple trajectory outputs and concentration ensembles.

Meteorological model preprocessing. HYSPLIT can use a large variety of meteorological model data in its calculations, ranging from mesoscale to global scales. Rather than having a different version of HYSPLIT to cope with the variations in variables and structure for each meteorological data source, a customized preprocessor is used to convert each meteorological data source into a HYSPLIT-compatible format. In this way HYSPLIT can easily be run with one or more meteorological datasets at the same time, using the optimal data for each calculation point. Table 2 describes some of the meteorological data already formatted for HYSPLIT that are publicly available from NOAA ARL (www.ready.noaa.gov/archives.php) and NOAA NCEP (ftp://ftpprd.ncep.noaa.gov//pub/data/nccf/com/hysplit/prod/). In addition, the following model outputs can also be used to drive HYSPLIT: the Weather Research and Forecasting (WRF) Model (Skamarock et al. 2008), MM5 (Grell et al. 1994), the Regional Atmospheric Modeling System (RAMS; Pielke et al. 1992), and the European Centre for Medium-Range Weather Forecasts (ECMWF) interim reanalysis (ERA-Interim; Dee et al. 2011).

Multiple trajectory analysis. The calculation of forward and backward trajectories allows for the depiction of airflow patterns to interpret the transport of pollutants over different spatial and temporal ranges. Frequently trajectories are used to track the airmass history or to forecast airmass movement and to account for the uncertainty in the associated wind patterns. Grouping trajectories that share some commonalities in space and time simplifies their analysis and interpretation and also reduces the uncertainty in the determination of the atmospheric transport pathways (Fleming et al. 2012).

Once the multiple trajectories representing the flow pattern of interest have been calculated, trajectories that are near each other can be merged into groups, called clusters, and represented by their mean trajectory. Differences between trajectories within a cluster are minimized while differences between clusters are maximized. Computationally, trajectories are combined until the total variance of the individual trajectories about their cluster-mean starts to increase substantially (Stunder 1996). This occurs when disparate clusters are combined. For references to cluster analysis methods the reader is referred to, for example, Borge et al. (2007), Karaca and Camci (2010), Markou and Kassomenos (2010), Baker (2010), and Cabello et al. (2008).

Concentration ensembles. The use of dispersion model ensembles—with the objective of improving plume simulations and assessing their uncertainty—has been an increasingly attractive approach to study atmospheric transport (e.g., Potempski et al. 2008; Lee et al. 2009; Solazzo et al. 2013; Stein et al. 2015). The HYSPLIT system has a built-in capability to produce three different simulation ensembles. This ensemble approach has been applied to case studies using different sets of initial conditions and internal model physical parameters (Draxler 2003; Stein et al. 2007; Chen et al. 2012). These built-in ensembles are not meant to be comprehensive and only account for some of the components of the concentration uncertainty, such as those arising from differences in initial conditions and model parameterizations. The first, called the "meteorological grid" ensemble, is created by slightly offsetting the meteorological data to test the sensitivity of the advection calculation to

the gradients in the meteorological data fields. The rationale for the shifting is to assess the effect that a limited spatial- and temporal-resolution meteorological data field—an approximation of the true flow field which is continuous in space and time—has on the output concentration (Draxler 2003). The second, called the "turbulence" ensemble, represents the uncertainty in the concentration calculation arising from the model's characterization of the random motions created by atmospheric turbulence (Stein et al. 2007). This ensemble is generated by varying the initial seed of the random number generator used to simulate the dispersive component of the motion of each particle. The model already estimates this turbulence when computing particle dispersal. However, normally, a sufficiently large number of particles would be released to ensure that each simulation gives similar results. In the turbulence ensemble approach, the number of particles released is reduced and multiple simulations are run, each with a different random number seed. The third, the "physics" ensemble, is built by varying key physical model parameters and model options such as the Lagrangian representation of the particles/puffs, Lagrangian time scales, and vertical and horizontal dispersion parameterizations.

MODEL EVALUATION USING TRACER EXPERIMENTS. Atmospheric tracer experiments offer a unique opportunity to evaluate the transport and dispersion independently from other model components such as chemical transformations or deposition. In these experiments, known amounts of an inert gas are emitted into the atmosphere and measured downwind for several days. One such experiment is the CAPTEX (Ferber et al. 1986) campaign that took place from 18 September to 29 October 1983 and consisted of six 3-h perfluro-monomethylcyclohexane (PMCH) releases: four from Dayton, Ohio, and two from Sudbury, Ontario, Canada. Samples were collected at 84 sites located 300–800 km downwind from the source at 3- and 6-h averaging periods for approximately 2–3 days after each release.

To illustrate how HYSPLIT's updates are evaluated, we performed a series of simulations using some of the updated vertical mixing parameterizations and compared the results with CAPTEX data. HYSPLIT was configured to simulate each of the six CAPTEX experiments by releasing 50 000 3D Lagrangian particles, using a vertical Lagrangian time scale (TL_w)—which is a measure of the persistence of fluid motion—of 5 and 200 s for stable and unstable conditions, respectively (see online supplement for further details), and employing an output concentration grid over the relevant domain with dimensions 0.25° × 0.25° by 100 m in depth. The fluxes of heat and momentum from the meteorological model were used to estimate the boundary layer stability parameters. All the HYSPLIT simulations used the meteorological data fields from the Advanced Research version of WRF (Skamarock et al. 2008), version 3.5. The innermost WRF domain was configured to cover the northeastern U.S. with a horizontal resolution of 9 km and 27 vertical layers using the Mellor–Yamada–Janjić (MYJ) (Janjić 1990) PBL scheme. The MYJ parameterization is a local, 1.5-order closure in which the TKE is a prognostic variable that is used for determining the diffusion coefficients. Moreover, as an alternative to the instantaneous wind fields generally used to drive the transport and dispersion simulations, WRF also produces time-averaged, mass-coupled, and horizontal and vertical velocities (Nehrkorn et al. 2010; Hegarty et al. 2013) that are automatically used by HYSPLIT if they are available.

Table 3. Statistical model performance measures for the six CAPTEX experiments. Values are given as rank, which is a normalized combination of the four statistics *R*, FB, FMS, and KSP [see Eq. (4) and text for details].

Run	Instantaneous winds (TKE)	Instantaneous winds (Kantha and Clayson 2000)	Time-averaged winds (Kantha and Clayson 2000)	Time-averaged winds (TKE)
CAPTEX-1	2.94	2.49	2.34	2.69
CAPTEX-2	2.79	3.11	3.24	2.90
CAPTEX-3	1.80	1.91	1.94	1.84
CAPTEX-4	2.14	2.31	2.14	2.18
CAPTEX-5	2.81	2.62	2.71	2.87
CAPTEX-7	2.37	2.36	2.64	2.48

Because of the difficulty in determining model performance using a single evaluation metric, we evaluate the model's performance against observations using the ranking method as defined by Draxler (2006). This method adds the correlation coefficient R, fractional bias (FB), figure of merit in space (FMS), and Kolmogorov–Smirnov parameter (KSP) into a single normalized Rank parameter that ranges from 0 to 4 (from worst to best); namely,

$$\text{Rank} = R^2 + 1 - |\text{FB}/2| + \text{FMS}/100 + (1 - \text{KSP}/100). \quad (4)$$

Table 3 shows the model performance for six CAPTEX releases using four different model configurations that combine two available mixing calculation options: one based on the horizontal and vertical friction velocities and the PBL height (Kantha and Clayson 2000) and another using TKE from WRF. These are combined with the use of snapshot or time-averaged mass-coupled wind fields. Note that no particular combination gives the best model performance for all the tracer releases, indicating that different parameterizations present an advantage or disadvantage under different atmospheric conditions. For example, Figs. 2a and 2b compare the simulated and observed tracer concentrations from CAPTEX tracer releases 2 and 7, showing that the model captures the characteristics of the geographical distribution and magnitude of measured PMCH concentrations. The reader is referred to Hegarty et al. (2013) for a more detailed and complete comparison with CAPTEX and additional tracer data. Other transport and dispersion models such as STILT (Lin et al. 2003) and Flexible Particle dispersion model (FLEXPART; Stohl et al. 2005) were compared in that work and showed similar performance.

We strongly believe that comparing with tracer experiments should be an integral part of the evaluation of transport and dispersion models. To facilitate this, we have made the CAPTEX data—along with an additional nine other tracer datasets (most consisting of multiple releases)—publically available from the Data Archive of Tracer Experiments and Meteorology (DATEM; www.arl.noaa.gov/DATEM.php) in a common format. DATEM also contains HYSPLIT simulation results for each experiment.

HYSPLIT TODAY. The HYSPLIT modeling system can be currently run on PC, Mac, or Linux platforms using a single processor. Multiple processor parallelized environment calculations based on a message passing interface (MPI) implementation are available for Mac and Linux. The system includes a suite of pre- and postprocessing programs to create input data as well as to visualize and analyze the simulation outputs. These programs can be called through a graphical user interface (GUI), the command line, or automated through scripts. The model is available for download at www.ready.noaa.gov/HYSPLIT.php. A registered version is also available that adds the

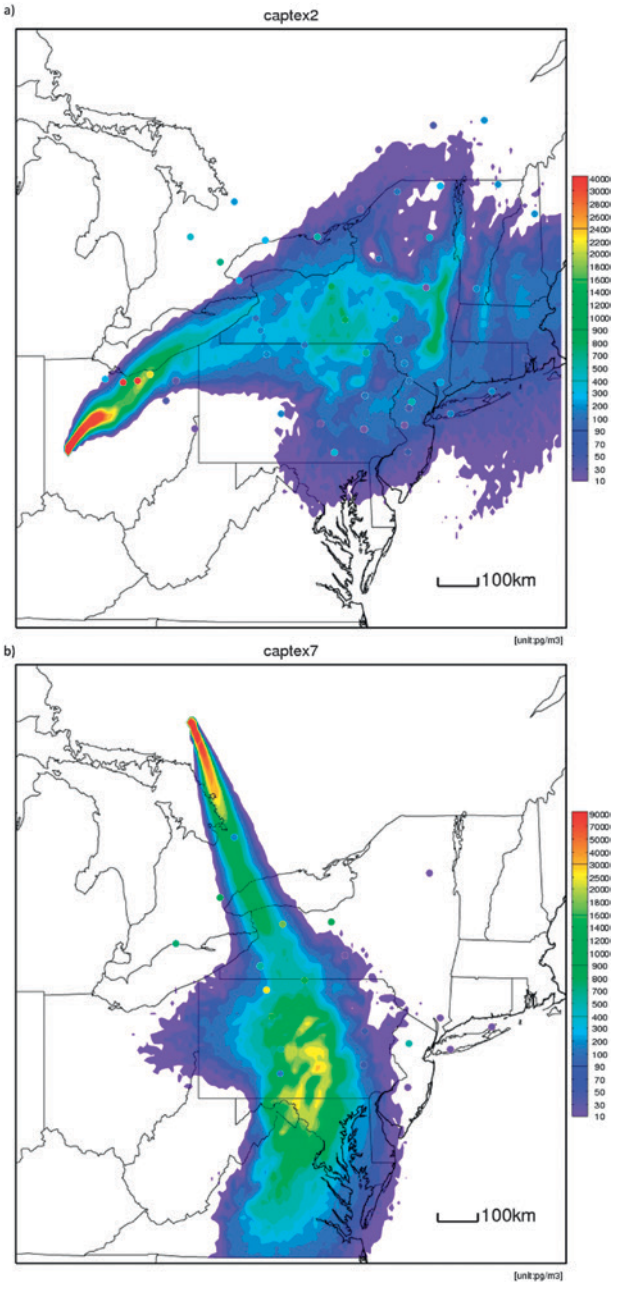

Fig. 2. Modeled (colored contours) and measured (colored circles) PMCH concentrations (pg m^{-3}) averaged over 48 h corresponding to (a) CAPTEX tracer release 2 from Dayton from 1700 to 2000 UTC 25 Sep 1983 and (b) CAPTEX tracer release 7 from Sudbury, Ontario, Canada, from 0600 to 0900 UTC 29 Oct 1983.

capability of running the model with current (today's) forecast meteorological data. About 3,000 registered users have already downloaded HYSPLIT. The source code is available upon request following the instructions to download the registered version.

Another way to gain public access to meteorological data and run HYSPLIT trajectory and dispersion simulations is through the Real-Time Environmental Applications and Display System (READY) (Rolph et al. 1993b), a web-based system developed and maintained by ARL (ready.arl.noaa.gov/). READY brings together the trajectory and dispersion model, graphical display programs, and textual forecast programs generated over many years at ARL into a particularly easy-to-use form. Since its initial development in 1997 (Fig. 1), thousands of users (about 80,000 HYSPLIT simulations per month) have generated products from READY for their day-to-day needs and research projects. In addition, a specialized website has been developed to allow NWS forecasters to run HYSPLIT for local events (e.g., hazardous materials incidents, forest fires, and nuclear accidents) and relay the results directly to state and local emergency managers through a customized web page.

Every year HYSPLIT developers offer training workshops on the installation and use of the modeling system, including a wide variety of applications such as volcanic eruptions, radionuclide accidents, dust storms, wildfire smoke, and tracer experiments. Training materials, including a self-paced tutorial, are available at www.arl.noaa.gov/HYSPLIT_workshop.php. Workshop participants typically include members of the U.S. and international governments, private industry, and academia. In addition, a forum for HYSPLIT model users is available to communicate questions, problems, and experiences (https://hysplitbbs.arl.noaa.gov/). This forum currently has more than 2,000 participants.

Many of the model applications described in this work are currently being used to fulfill ARL's mission. One of the many functions of ARL is to provide atmospheric transport and dispersion information and related research to NOAA, other federal agencies, and the general public in order to estimate the consequences of atmospheric releases of pollutants, radioactivity, and other potentially harmful materials.

For example, ARL's volcanic ash model [initially Volcanic Ash Forecast Transport and Dispersion (VAFTAD; Heffter and Stunder 1993); now HYSPLIT (Stunder et al. 2007)] (Fig. 3) provides critical information on plume transport and dispersion to the aviation industry (www.ready.noaa.gov/READYVolcAsh.php). HYSPLIT is currently run operationally by the NOAA/NWS to forecast the transport and dispersion of volcanic ash in and near the U.S. Volcanic Ash Advisory Centers' (VAAC) areas of responsibility covering North and Central America. Meteorologists at the VAAC and the Meteorological Watch Offices use the HYSPLIT forecasts, among other sources of information, for writing Volcanic Ash Advisories and Significant Meteorological Information warning messages (called SIGMETs). The HYSPLIT dispersion forecasts are issued to the public and made available online, such as at the NWS Aviation Weather Center (http://aviationweather.gov/iffdp/volc). Additional volcanic ash applications of the model include HYSPLIT's participation in a dispersion model intercomparison among the international centers that provide advisories for

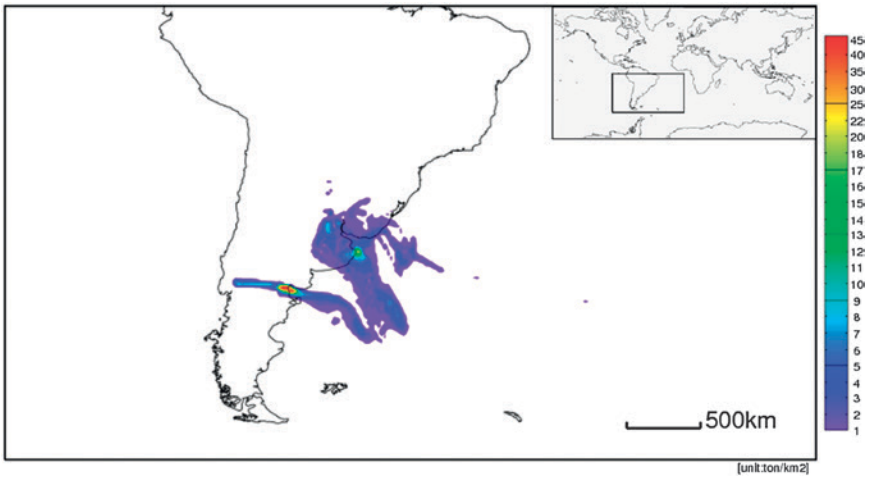

Fig. 3. Example of the calculated ash column corresponding to the eruption of the Cordón Caulle volcano in South America for 0600 UTC 8 Jun 2011. For this illustration, a total of 25 million 3D particles were released from 4 to 20 Jun 2011 and transported/dispersed using the GDAS meteorological dataset. The source term is based on an empirical formula that relates the height of the eruption column to the mass eruption rate (Mastin et al. 2009). The height of the eruption column is estimated from Collini et al. (2013). We assume a particle distribution based on four size bins (Heffter and Stunder 1993). More details about volcanic ash simulations can be found at www.arl.noaa.gov/HYSPLIT_ashinterp.php**.**

aviation (Witham et al. 2007), investigating source-term sensitivity (Webley et al. 2009), locating the volcano source given downwind ash–aircraft encounters (Tupper et al. 2006), and modeling VOG (a mixture of SO_2 and sulfate) in Hawaii (http://mkwc.ifa.hawaii.edu/vmap/index.cgi).

As a result of communications difficulties between countries following the Chernobyl accident in the spring of 1986, the World Meteorological Organization (WMO) was requested by the International Atomic Energy Agency (IAEA) and other international organizations to arrange for early warning messages about nuclear accidents to be transmitted over the Global Telecommunications System. In addition, some WMO member countries lacking extensive forecasting capability requested specialized pollutant transport and dispersion forecasts during these emergencies. Consequently, Regional Specialized Meteorological Centers (RSMCs; www.wmo.int/pages/prog/www/DPFSERA/EmergencyResp.html) were set up to respond to these needs. ARL, together with NOAA's NCEP, constitute the Washington RSMC for transport and dispersion products through WMO. RSMC Washington, along with RSMC Montreal (operated by the Canadian Meteorological Centre), provide meteorological guidance and dispersion predictions using their respective models in the event of an atmospheric release of radioactive or hazardous materials crossing international boundaries in North, Central, and South America (www.arl.noaa.gov/rsmc.php). Furthermore, HYSPLIT was used to evaluate the consequences of the accidental release of nuclear material into the atmosphere from the Fukushima Daiichi Nuclear Power Plant following an earthquake and tsunami in March 2011 (e.g., Fig. 4; Draxler and Rolph 2012; Draxler et al. 2013).

Transport of forest fire smoke and its effect on weather has been a topic of NOAA interest at least since the middle of the last century (Smith 1950) and modeling the movement of smoke from large wildfires has been an ongoing development activity of ARL since 1998 (Rolph et al. 2009). This research eventually led to the first operational smoke forecasts over the continental U.S. in 2007 by NOAA in support of the National Air Quality Forecast Capability (Rolph et al. 2009) (www.arl.noaa.gov/smoke.php). Today, in addition to the continental United States, smoke forecasts are produced for Alaska and Hawaii on a daily basis to provide guidance to air quality forecasters and the public on the levels of particulate matter with diameters smaller than 2.5 μm ($PM_{2.5}$) in the air (http://airquality.weather.gov/).

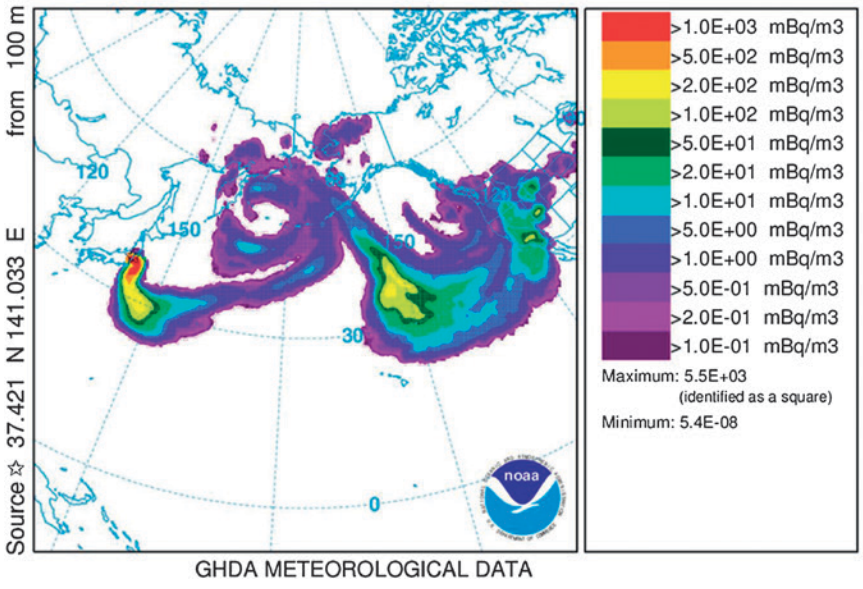

Fig. 4. Illustration of particulate cesium-137 concentrations originated from the Fukushima Daiichi reactor. See Draxler and Rolph (2012) for further details.

Finally, HYSPLIT has very recently been coupled inline to WRF (Ngan et al. 2015) taking advantage of the higher temporal frequency available from the meteorological data. The model runs within the WRF architecture using the same spatial and temporal resolution and it has been tested against CAPTEX and other tracer experiments. This is a very promising approach for applications influenced by rapidly changing conditions and/or complex terrain. Further evaluation of this approach is underway.

ACKNOWLEDGMENTS. The authors thank Hyun-Cheol Kim for help with graphics and Dian Seidel for very helpful editorial comments. We also thank the many model users that have contributed to the development and improvement of HYSPLIT over the past three decades.

REFERENCES

Angell, J. K., D. H. Pack, G. C. Holzworth, and C. R. Dickson, 1966: Tetroon trajectories in an

urban atmosphere. *J. Appl. Meteor.*, **5**, 565–572, doi:10.1175/1520-0450(1966)005<0565:TTIAUA>2.0.CO;2.

——, ——, L. Machta, C. R. Dickson, and W. H. Hoecker, 1972: Three-dimensional air trajectories determined from tetroon-flights in the planetary boundary layer of the Los Angeles Basin. *J. Appl. Meteor.*, **11**, 451–471, doi:10.1175/1520-0450(1972)011<0451:TDATDF>2.0.CO;2.

——, C. R. Dickson, and W. H. Hoecker Jr., 1976: Tetroon trajectories in the Los Angeles Basin defining the source of air reaching the San Bernardino-Riverside area in late afternoon. *J. Appl. Meteor.*, **15**, 197–204, doi:10.1175/1520-0450(1976)015<0197:TTITLA>2.0.CO;2.

Ashrafi, K., M. Shafiepour-Motlagh, A. Aslemand, and S. Ghader, 2014: Dust storm simulation over Iran using HYSPLIT. *J. Environ. Health Sci. Eng.*, **12**, 9, doi:10.1186/2052-336X-12-9.

Azzi, M., G. M. Johnson, R. Hyde, and M. Young, 1995: Prediction of NO_2 and O_3 concentrations for NO_X plumes photochemically reacting in urban air. *Math. Comput. Modell.*, **21**, 39–48, doi:10.1016/0895-7177(95)00050-C.

Baker, J., 2010: A cluster analysis of long range air transport pathways and associated pollutant concentrations within the UK. *Atmos. Environ.*, **44**, 563–571, doi:10.1016/j.atmosenv.2009.10.030.

Barad, M. L., Ed., 1958: Project Prairie Grass—A field program in diffusion. Vols. I and II. Air Force Cambridge Research Center Geophysical Research Paper 59, NTID PB 151424, PB 1514251, 439 pp.

Becker, A., and Coauthors, 2007: Global backtracking of anthropogenic radionuclides by means of a receptor oriented ensemble dispersion modelling system in support of Nuclear-Test-Ban Treaty verification. *Atmos. Environ.*, **41**, 4520–4534, doi:10.1016/j.atmosenv.2006.12.048.

Black, T., 1994: The new NMC mesoscale Eta model: Description and forecast examples. *Wea. Forecasting*, **9**, 265–278, doi:10.1175/1520-0434(1994)009<0265:TNNMEM>2.0.CO;2.

Borge, R., J. Lumbreras, S. Vardoulakis, P. Kassomenos, and E. Rodriguez, 2007: Analysis of long-range transport influences on urban PM10 using two stage atmospheric trajectory clusters. *Atmos. Environ.*, **41**, 4434–4450, doi:10.1016/j.atmosenv.2007.01.053.

Bowyer, T. W., R. Kephart, P. W. Eslinger, J. I. Friese, H. S. Miley, and P. R. J. Saey, 2013: Maximum reasonable radioxenon releases from medical isotope production facilities and their effect on monitoring nuclear explosions. *J. Environ. Radioact.*, **115**, 192–200, doi:10.1016/j.jenvrad.2012.07.018.

Cabello, M., J. A. G. Orza, and V. Galiano, 2008: Air mass origin and its influence over the aerosol size distribution: A study in SE Spain. *Adv. Sci. Res.*, **2**, 47–52, doi:10.5194/asr-2-47-2008.

Challa, V. S., and Coauthors, 2008: Sensitivity of atmospheric dispersion simulations by HYSPLIT to the meteorological predictions from a meso-scale model. *Environ. Fluid Mech.*, **8**, 367–387, doi:10.1007/s10652-008-9098-z.

Chen, B., A. F. Stein, N. Castell, J. D. de la Rosa, A. M. Sanchez de la Campa, Y. Gonzalez-Castanedo, and R. R. Draxler, 2012: Modeling and surface observations of arsenic dispersion from a large Cu-smelter in southwestern Europe. *Atmos. Environ.*, **49**, 114–122, doi:10.1016/j.atmosenv.2011.12.014.

——, ——, P. Guerrero Maldonado, A. M. Sanchez de la Campa, Y. Gonzalez-Castanedo, N. Castell, and J. D. de la Rosa, 2013: Size distribution and concentrations of heavy metals in atmospheric aerosols originating from industrial emissions as predicted by the HYSPLIT model. *Atmos. Environ.*, **71**, 234–244, doi:10.1016/j.atmosenv.2013.02.013.

Chock, D. P., and S. L. Winkler, 1994a: A particle grid air quality modeling approach: 1. The dispersion aspect. *J. Geophys. Res.*, **99** (D1), 1019–1031, doi:10.1029/93JD02795.

——, and ——, 1994b: A particle grid air quality modeling approach: 2. Coupling with chemistry. *J. Geophys. Res.*, **99** (D1), 1033–1041, doi:10.1029/93JD02796.

Cohen, M., B. Commoner, H. Eisl, P. W. Bartlett, A. Dickar, C. Hill, J. Quigley, and J. Rosenthal, 1995: Quantitative estimation of the entry of dioxins, furans and hexachlorobenzene into the Great Lakes from airborne and waterborne sources. Queens College Center for the Biology of Natural Systems Rep., 115 pp. [Available online at www.arl.noaa.gov/documents/reports/Great_Lakes_Dioxin_HCB_Report_1995.pdf.]

——, ——, P. W. Bartlett, P. Cooney, and H. Eisl, 1997a: Exposure to endocrine disruptors from long range air transport of pesticides. CBNS, Queens College, CUNY Rep. to the W. Alton Jones Foundation, 66 pp. [Available online www.arl.noaa.gov/data/web/reports/cohen/atrazine_report.pdf.]

——, ——, ——, H. Eisl, C. Hill, and J. Rosenthal, 1997b: Development and application of an air transport model for dioxins and furans. *Organohalogen Compd.*, **33**, 214–219.

——, and Coauthors, 2002: Modeling the atmospheric transport and deposition of PCDD/F to the Great Lakes. *Environ. Sci. Technol.*, **36**, 4831–4845, doi:10.1021/es0157292.

——, and Coauthors, 2004: Modeling the atmospheric transport and deposition of mercury to the Great

Lakes. *Environ. Res.*, **95**, 247–265, doi:10.1016/j.envres.2003.11.007.

——, R. Draxler, and R. Artz, 2011: Modeling atmospheric mercury deposition to the Great Lakes. NOAA Air Resources Laboratory Final Rep. for work conducted with FY2010 funding from the Great Lakes Restoration Initiative, 160 pp. [Available online www.arl.noaa.gov/documents/reports/GLRI_FY2010_Atmospheric_Mercury_Final_Report_2011_Dec_16.pdf.]

——, ——, and ——, 2013: Modeling atmospheric mercury deposition to the Great Lakes: Examination of the influence of variations in model inputs, parameters, and algorithms on model results. NOAA Air Resources Laboratory Final Rep. for work conducted with FY2011 funding from the Great Lakes Restoration Initiative, 157 pp. [Available online at www.arl.noaa.gov/documents/reports/GLRI_FY2011_Atmospheric_Mercury_Final_Report_2013_June_30.pdf.]

——, ——, and ——, 2014: Modeling atmospheric mercury deposition to the Great Lakes: Projected consequences of alternative future emissions scenarios. NOAA Air Resources Laboratory Final Rep. for work conducted with FY2012 funding from the Great Lakes Restoration Initiative, 193 pp. [Available online at www.arl.noaa.gov/documents/reports/GLRI_FY2012_Atmos_Mercury_09_Oct_2014.pdf.]

Collini, E., M. S. Osores, A. Folch, J. G. Viramonte, G. Villarosa, and G. Salmuni, 2013: Volcanic ash forecast during the June 2011 Cordón Caulle eruption. *Nat. Hazards*, **66**, 389–412, doi:10.1007/s11069-012-0492-y.

Connan, O., K. Smith, C. Organo, L. Solier, D. Maro, and D. Hébert, 2013: Comparison of RIMPUFF, HYSPLIT, ADMS atmospheric dispersion model outputs, using emergency response procedures, with ^{85}Kr measurements made in the vicinity of nuclear reprocessing plant. *J. Environ. Radioact.*, **124**, 266–277, doi:10.1016/j.jenvrad.2013.06.004.

Dee, D. P., and Coauthors, 2011: The ERA-Interim reanalysis: Configuration and performance of the data assimilation system. *Quart. J. Roy. Meteor. Soc.*, **137**, 553–597, doi:10.1002/qj.828.

Ding, A., T. Wang, and C. Fu, 2013: Transport characteristics and origins of carbon monoxide and ozone in Hong Kong, South China. *J. Geophys. Res. Atmos.*, **118**, 9475–9488, doi:10.1002/jgrd.50714.

Draxler, R. R., 1982: Measuring and modeling the transport and dispersion of kRYPTON-85 1500km from a point source. *Atmos. Environ.*, **16**, 2763–2776, doi:10.1016/0004-6981(82)90027-0.

——, 1987: Sensitivity of a trajectory model to the spatial and temporal resolution of the meteorological data during CAPTEX. *J. Climate Appl. Meteor.*, **26**, 1577–1588, doi:10.1175/1520-0450(1987)026<1577:SOATMT>2.0.CO;2.

——, 1992: Hybrid Single-Particle Lagrangian Integrated Trajectories (HY-SPLIT): Version 3.0—User's guide and model description. Air Resources Laboratory Tech. Memo. ERL ARL-195, 84 pp. [Available online at www.arl.noaa.gov/documents/reports/ARL%20TM-195.pdf.]

——, 2000: Meteorological factors of ozone predictability at Houston, Texas. *J. Air Waste Manag. Assoc.*, **50**, 259–271, doi:10.1080/10473289.2000.10463999.

——, 2003: Evaluation of an ensemble dispersion calculation. *J. Appl. Meteor.*, **42**, 308–317, doi:10.1175/1520-0450(2003)042<0308:EOAEDC>2.0.CO;2.

——, 2006: The use of global and mesoscale meteorological model data to predict the transport and dispersion of tracer plumes over Washington, D.C. *Wea. Forecasting*, **21**, 383–394, doi:10.1175/WAF926.1.

——, 2007: Demonstration of a global modeling methodology to determine the relative importance of local and long-distance sources. *Atmos. Environ.*, **41**, 776–789, doi:10.1016/j.atmosenv.2006.08.052.

——, and A. D. Taylor, 1982: Horizontal dispersion parameters for long-range transport modeling. *J. Appl. Meteor.*, **21**, 367–372, doi:10.1175/1520-0450(1982)021<0367:HDPFLR>2.0.CO;2.

——, and B. J. B. Stunder, 1988: Modeling the CAPTEX vertical tracer concentration profiles. *J. Appl. Meteor.*, **27**, 617–625, doi:10.1175/1520-0450(1988)027<0617:MTCVTC>2.0.CO;2.

——, and J. L. Heffter, Eds., 1989: Across North America Tracer Experiment (ANATEX) volume I: Description, ground-level sampling at primary sites, and meteorology. NOAA Tech. Memo. ERL ARL-167. [Available online at www.arl.noaa.gov/documents/reports/arl-167.pdf.]

——, and G. D. Hess, 1997: Description of the HYSPLIT_4 modeling system. NOAA Tech. Memo. ERL ARL-224, 24 pp. [Available online at www.arl.noaa.gov/documents/reports/arl-224.pdf.]

——, and G. D. Hess, 1998: An overview of the HYSPLIT_4 modeling system for trajectories, dispersion, and deposition. *Aust. Meteor. Mag.*, **47**, 295–308.

——, and G. D. Rolph, 2012: Evaluation of the Transfer Coefficient Matrix (TCM) approach to model the atmospheric radionuclide air concentrations from Fukushima. *J. Geophys. Res.*, **117**, D05107, doi:10.1029/2011JD017205.

——, P. Ginoux, and A. F. Stein, 2010: An empirically derived emission algorithm for wind-

blown dust. *J. Geophys. Res.*, **115**, D16212, doi:10.1029/2009JD013167.

——, and Coauthors, 2013: World Meteorological Organization's model simulations of the radionuclide dispersion and deposition from the Fukushima Daiichi nuclear power plant accident. *J. Environ. Radioact.*, **139**, 172–184, doi:10.1016/j.jenvrad.2013.09.014.

Efstathiou, C., S. Isukapalli, and P. Georgopoulos, 2011: A mechanistic modeling system for estimating large-scale emissions and transport of pollen and co-allergens. *Atmos. Environ.*, **45**, 2260–2276, doi:10.1016/j.atmosenv.2010.12.008.

Escudero, M., A. Stein, R. R. Draxler, X. Querol, A. Alastuey, S. Castillo, and A. Avila, 2006: Determination of the contribution of northern Africa dust source areas to PM10 concentrations over the central Iberian Peninsula using the Hybrid Single-Particle Lagrangian Integrated Trajectory model (HYSPLIT) model. *J. Geophys. Res.*, **111**, D06210, doi:10.1029/2005JD006395.

——, ——, ——, ——, ——, ——, and ——, 2011: Source apportionment for African dust outbreaks over the Western Mediterranean using the HYSPLIT model. *Atmos. Res.*, **99** (3–4), 518–527, doi:10.1016/j.atmosres.2010.12.002.

Fay, B., H. Glaab, I. Jacobsen, and R. Schrodin, 1995: Evaluation of Eulerian and Lagrangian atmospheric transport models at the Deutscher Wetterdienst using ANATEX surface tracer data. *Atmos. Environ.*, **29**, 2485–2497, doi:10.1016/1352-2310(95)00144-N.

Ferber, G. J., J. L. Heffter, R. R. Draxler, R. J. Lagomarsino, F. L. Thomas, and R. N. Dietz, 1986: Cross-Appalachian Tracer Experiment (CAPTEX '83) Final Report. Air Resources Laboratory NOAA Tech. Memo. ERL ARL-142, 60 pp. [Available online at www.arl.noaa.gov/documents/reports/arl-142.pdf.]

Fleming, Z. L., P. S. Monks, and A. J. Manning, 2012: Review: Untangling the influence of air-mass history in interpreting observed atmospheric composition. *Atmos. Res.*, **104–105**, 1–39, doi:10.1016/j.atmosres.2011.09.009.

Gaiero, D. M., and Coauthors, 2013: Ground/satellite observations and atmospheric modeling of dust storms originated in the high Puna-Altiplano deserts (South America): Implications for the interpretation of paleo-climatic archives. *J. Geophys. Res.*, **118**, 3817–3831, doi:10.1002/jgrd.50036.

Gasso, S., and A. F. Stein, 2007: Does dust from Patagonia reach the sub-Antarctic Atlantic Ocean? *Geophys. Res. Lett.*, **34**, L01801, doi:10.1029/2006GL027693.

Gerbig, C., J. C. Lin, S. C. Wofsy, B. C. Daube, A. E. Andrews, B. B. Stephens, P. S. Bakwin, and C. A. Grainger, 2003: Toward constraining regional-scale fluxes of CO_2 with atmospheric observations over a continent: 2. Analysis of COBRA data using a receptor-oriented framework. *J. Geophys. Res.*, **108**, 4757, doi:10.1029/2003JD003770.

Gery, M. W., G. Z. Whitten, J. P. Killus, and M. C. Dodge, 1989: A photochemical kinetics mechanism for urban and regional scale computer modeling. *J. Geophys. Res.*, **94** (D10), 12 925–12 956, doi:10.1029/JD094iD10p12925.

Gifford, F. A., 1961: Use of routine meteorological observations for estimating atmospheric dispersion. *Nucl. Saf.*, **2**, 47–51.

Grell, G. A., J. Dudhia, and D. R. Stauffer, 1994: A description of the fifth-generation Penn State/NCAR Mesoscale Model (MM5). NCAR Tech. Note NCAR/TN-398+STR, 122 pp. [Available online at http://nldr.library.ucar.edu/repository/assets/technotes/TECH-NOTE-000-000-000-214.pdf.]

Han, Y. J., T. M. Holsen, P. K. Hopke, and S. M. Yi, 2005: Comparison between back-trajectory based modeling and Lagrangian backward dispersion modeling for locating sources of reactive gaseous mercury. *Environ. Sci. Technol.*, **39**, 1715–1723, doi:10.1021/es0498540.

Heffter, J. L., and B. J. B. Stunder, 1993: Volcanic Ash Forecast Transport And Dispersion (VAFTAD) model. *Wea. Forecasting*, **8**, 533–541, doi:10.1175/1520-0434(1993)008<0533:VAFTAD>2.0.CO;2.

——, A. D. Taylor, and G. J. Ferber, 1975: A regional-continental scale transport, diffusion, and deposition model. Part I: Trajectory model. Part II: Diffusion-deposition models. Air Resources Laboratories Tech. Memo. ERL ARL-50, 28 pp. [Available online at www.arl.noaa.gov/documents/reports/ARL-50.PDF.]

Hegarty, J., and Coauthors, 2013: Evaluation of Lagrangian particle dispersion models with measurements from controlled tracer releases. *J. Appl. Meteor. Climatol.*, **52**, 2623–2637, doi:10.1175/JAMC-D-13-0125.1.

Hoke, J. E., N. A. Phillips, G. J. DiMego, J. J. Tuccillo, and J. G. Sela, 1989: The regional analysis and forecast system of the National Meteorological Center. *Wea. Forecasting*, **4**, 323–334, doi:10.1175/1520-0434(1989)004<0323:TRAAFS>2.0.CO;2.

Janjić, Z. I., 1990: The step-mountain coordinate: Physical package. *Mon. Wea. Rev.*, **118**, 1429–1443, doi:10.1175/1520-0493(1990)118<1429:TSMCPP>2.0.CO;2.

——, 2003: A nonhydrostatic model based on a new approach. *Meteor. Atmos. Phys.*, **82**, 271–285, doi:10.1007/s00703-001-0587-6.

——, T. Black, M. Pyle, E. Rogers, H.-Y. Chuang, and G. DiMego, 2005: High resolution applications of

the WRF NMM. *21st Conf. on Weather Analysis and Forecasting/17th Conf. on Numerical Weather Prediction*, Washington, DC, Amer. Meteor. Soc., 16A.4. [Available online at https://ams.confex.com/ams/WAFNWP34BC/techprogram/paper_93724.htm.]

Jeong, H., M. Park, H. Jeong, W. Hwang, E. Kim, and M. Han, 2013: Radiological risk assessment caused by RDD terrorism in an urban area. *Appl. Radiat. Isot.*, **79**, 1–4, doi:10.1016/j.apradiso.2013.04.018.

Jeong, S., Y.-K. Hsu, A. E. Andrews, L. Bianco, P. Vaca, J. M. Wilczak, and M. L. Fischer, 2013: A multitower measurement network estimate of California's methane emissions. *J. Geophys. Res.*, **118**, 11 339–11 351, doi:10.1002/jgrd.50854.

Johnson, G. M., 1984: A simple model for predicting the ozone concentration of ambient air. *Proc. Eighth Int. Clean Air Conf.*, Melbourne, Victoria, Australia, Clean Air Society of Australia and New Zealand, 715–731.

Kalnay, E., and Coauthors, 1996: The NCEP/NCAR 40-Year Reanalysis Project. *Bull. Amer. Meteor. Soc.*, **77**, 437–471, doi:10.1175/1520-0477(1996)077<0437:TNYRP>2.0.CO;2.

Kanamitsu, M., 1989: Description of the NMC Global Data Assimilation and Forecast System. *Wea. Forecasting*, **4**, 335–342, doi:10.1175/1520-0434(1989)004<0335:DOTNGD>2.0.CO;2.

Kang, D., B. K. Eder, A. F. Stein, G. Grell, S. E. Peckham, and J. McHenry, 2005: The New England Air Quality Forecasting Pilot Program: Development of an evaluation protocol and performance benchmark. *J. Air Waste Manag. Assoc.*, **55**, 1782–1796, doi:10.1080/10473289.2005.10464775.

Kantha, L. H., and C. A. Clayson, 2000: *Small Scale Processes in Geophysical Fluid Flows.* International Geophysics, Vol. 67, Academic Press, 750 pp.

Karaca, F., and F. Camci, 2010: Distant source contributions to PM10 profile evaluated by SOM based cluster analysis of air mass trajectory sets. *Atmos. Environ.*, **44**, 892–899, doi:10.1016/j.atmosenv.2009.12.006.

Kinoshita, N., and Coauthors, 2011: Assessment of individual radionuclide distributions from the Fukushima nuclear accident covering central-east Japan. *Proc. Natl. Acad. Sci. USA*, **108**, 19 526–19 529, doi:10.1073/pnas.1111724108.

Kinser, A. M., 2001: Simulating wet deposition of radiocesium from the Chernobyl accident. M.S. thesis, Graduate School of Engineering and Management, Air Force Institute of Technology, 108 pp. [Available online at www.dtic.mil/get-tr-doc/pdf?AD=ADA392534.]

Kort, E. A., and Coauthors, 2008: Emissions of CH_4 and N_2O over the United States and Canada based on a receptor-oriented modeling framework and COBRA-NA atmospheric observations. *Geophys. Res. Lett.*, **35**, L18808, doi:10.1029/2008GL034031.

Leadbetter, S. L., M. C. Hort, A. R. Jones, H. N. Webster, and R. R. Draxler, 2015: Sensitivity of the modelled deposition of Caesium-137 from the Fukushima Dai-ichi nuclear power plant to the wet deposition parameterisation in NAME. *J. Environ. Radioact.*, **139**, 200–211, doi:10.1016/j.jenvrad.2014.03.018.

Lee, J. A., L. J. Peltier, S. E. Haupt, J. C. Wyngaard, D. R. Stauffer, and A. Deng, 2009: Improving SCIPUFF dispersion forecasts with NWP ensembles. *J. Appl. Meteor. Climatol.*, **48**, 2305–2319, doi:10.1175/2009JAMC2171.1.

Lin, J. C., C. Gerbig, S. C. Wofsy, A. E. Andrews, B. C. Daube, K. J. Davis, and C. A. Grainger, 2003: A near-field tool for simulating the upstream influence of atmospheric observations: The Stochastic Time-Inverted Lagrangian Transport (STILT) model. *J. Geophys. Res.*, **108**, 4493, doi:10.1029/2002JD003161.

Machta, L., 1992: Finding the site of the first Soviet nuclear test in 1949. *Bull. Amer. Meteor. Soc.*, **73**, 1797–1806, doi:10.1175/1520-0477(1992)073<1797:FTSOTF>2.0.CO;2.

Markou, M. T., and P. Kassomenos, 2010: Cluster analysis of five years of back trajectories arriving in Athens, Greece. *Atmos. Res.*, **98**, 438–457, doi:10.1016/j.atmosres.2010.08.006.

Mastin, L. G., and Coauthors, 2009: A multidisciplinary effort to assign realistic source parameters to models of volcanic ash-cloud transport and dispersion during eruptions. *J. Volcanol. Geotherm. Res.*, **186**, 10–21, doi:10.1016/j.jvolgeores.2009.01.008.

Mesinger, F., and Coauthors, 2006: North American Regional Reanalysis. *Bull. Amer. Meteor. Soc.*, **87**, 343–360, doi:10.1175/BAMS-87-3-343.

Moroz, B. E., H. L. Beck, A. Bouville, and S. L. Steven, 2010: Predictions of dispersion and deposition of fallout from nuclear testing using the NOAA-Hysplit Meteorological Model. *Health Phys.*, **99**, 252–269, doi:10.1097/HP.0b013e3181b43697.

Nehrkorn, T., J. Eluszkiewicz, S. C. Wofsy, J. C. Lin, C. Gerbig, M. Longo, and S. Freitas, 2010: Coupled Weather Research and Forecasting–Stochastic Time-Inverted Lagrangian Transport (WRF–STILT) model. *Meteor. Atmos. Phys.*, **107**, 51–64, doi:10.1007/s00703-010-0068-x.

Ngan, F., A. Stein, and R. Draxler, 2015: Inline coupling of WRF–HYSPLIT: Model development and evaluation using tracer experiments. *J. Appl. Meteor. Climatol.*, **54**, 1162–1176, doi:10.1175/JAMC-D-14-0247.1.

Pasken, R., and J. A. Pietrowicz, 2005: Using dispersion and mesoscale meteorological models to forecast pol-

len concentrations. *Atmos. Environ.*, **39**, 7689–7701, doi:10.1016/j.atmosenv.2005.04.043.

Pasquill, F., 1961: The estimation of the dispersion of windborne material. *Meteor. Mag.*, **90**, 33–49.

Philips, N. A., 1979: The nested grid model. NOAA/National Weather Service Tech. Rep. NWS-22, 80 pp.

Pielke, R. A., and Coauthors, 1992: A comprehensive meteorological modeling system—RAMS. *Meteor. Atmos. Phys.*, **49** (1–4), 69–91, doi:10.1007/BF01025401.

Potempski, S., and Coauthors, 2008: Multi-model ensemble analysis of the ETEX-2 experiment. *Atmos. Environ.*, **42**, 7250–7265, doi:10.1016/j.atmosenv.2008.07.027.

Rolph, G. D., R. R. Draxler, and R. G. de Pena, 1992: Modeling sulfur concentrations and depositions in the United States during ANATEX. *Atmos. Environ.*, **26A**, 73–93, doi:10.1016/0960-1686(92)90262-J.

——, ——, and ——, 1993a: The use of model-derived and observed precipitation in long-term sulfur concentration and deposition modeling. *Atmos. Environ.*, **27A**, 2017–2037, doi:10.1016/0960-1686(93)90275-4.

——, J. McQueen, and R. R. Draxler, 1993b: Real-Time Environmental Applications and Display sYstem (READY). *Proc. Topical Meeting on Environmental Transport and Dosimetry*, Charleston, SC, American Nuclear Society, 113–116.

——, and Coauthors, 2009: Description and verification of the NOAA Smoke Forecasting System: The 2007 fire season. *Wea. Forecasting*, **24**, 361–378, doi:10.1175/2008WAF2222165.1.

——, F. Ngan, and R. R. Draxler, 2014: Modeling the fallout from stabilized nuclear clouds using the HYSPLIT atmospheric dispersion model. *J. Environ. Radioact.*, **136**, 41–55, doi:10.1016/j.jenvrad.2014.05.006.

Ryaboshapko, A., and Coauthors, 2007a: Intercomparison study of atmospheric mercury models: 1. Comparison of models with short-term measurements. *Sci. Total Environ.*, **376**, 228–240, doi:10.1016/j.scitotenv.2007.01.072.

——, and Coauthors, 2007b: Intercomparison study of atmospheric mercury models: 2. Modelling results vs. long-term observations and comparison of country deposition budgets. *Sci. Total Environ.*, **377**, 319–333, doi:10.1016/j.scitotenv.2007.01.071.

Schaum, J., and Coauthors, 2010: Screening level assessment of risks due to dioxin emissions from burning oil from the BP Deep Water Horizon Gulf of Mexico spill. *Environ. Sci. Technol.*, **44**, 9383–9389, doi:10.1021/es103559w.

Skamarock, W. C., and Coauthors, 2008: A description of the Advanced Research WRF version 3. NCAR Tech. Note NCAR/TN-475+STR, 113 pp. [Available online at www.mmm.ucar.edu/wrf/users/docs/arw_v3_bw.pdf.]

Slade, D. H., 1966: Estimates of dispersion from pollutant releases of a few seconds to 8 hours in duration. Air Resources Laboratories Tech. Note 39-ARL-3, 26 pp. [Available online at www.arl.noaa.gov/documents/reports/TN-39-ARL-3.PDF.]

——, Ed., 1968: Meteorology and atomic energy 1968. Air Resources Laboratory, ESSA, for USAEC Division of Technical Information, 445 pp.

Smith, C. D., 1950: The widespread smoke layer from Canadian forest fires during late September 1950. *Mon. Wea. Rev.*, **78**, 180–184, doi:10.1175/1520-0493(1950)078<0180:TWSLFC>2.0.CO;2.

Solazzo, E., A. Riccio, I. Kioutsioukis, and S. Galmarini, 2013: Pauci ex tanto numero: Reduce redundancy in multi-model ensembles. *Atmos. Chem. Phys.*, **13**, 8315–8333, doi:10.5194/acp-13-8315-2013.

——, R. Venkatesan, R. Baskaran, V. Rajagopal, and B. Venkatraman, 2012: Regional scale atmospheric dispersion simulation of accidental releases of radionuclides from Fukushima Dai-ichi reactor. *Atmos. Environ.*, **61**, 66–84, doi:10.1016/j.atmosenv.2012.06.082.

Start, G. E., and L. L. Wendell, 1974: Regional effluent dispersion calculations considering spatial and temporal meteorological variations. Air Resources Laboratories Tech. Memo. ERL TM-ARL-44, 63 pp. [Available online at www.arl.noaa.gov/documents/reports/ARL-44.PDF.]

Stein, A. F., D. Lamb, and R. R. Draxler, 2000: Incorporation of detailed chemistry into a three-dimensional Lagrangian–Eulerian hybrid model: Application to regional tropospheric ozone. *Atmos. Environ.*, **34**, 4361–4372, doi:10.1016/S1352-2310(00)00204-1.

——, V. Isakov, J. Godowitch, and R. R. Draxler, 2007: A hybrid modeling approach to resolve pollutant concentrations in an urban area. *Atmos. Environ.*, **41**, 9410–9426, doi:10.1016/j.atmosenv.2007.09.004.

——, G. D. Rolph, R. R. Draxler, B. Stunder, and M. Ruminski, 2009: Verification of the NOAA Smoke Forecasting System: Model sensitivity to the injection height. *Wea. Forecasting*, **24**, 379–394, doi:10.1175/2008WAF2222166.1.

——, Y. Wang, J. D. de la Rosa, A. M. Sanchez de la Campa, N. Castell, and R. R. Draxler, 2011: Modeling PM10 originated from dust intrusions in the southern Iberian Peninsula using HYSPLIT. *Wea. Forecasting*, **26**, 236–242, doi:10.1175/WAF-D-10-05044.1.

——, F. Ngan, R. R. Draxler, and T. Chai, 2015: Potential use of transport and dispersion model ensembles for forecasting applications. *Wea. Forecasting*, **30**, 639–655, doi:10.1175/WAF-D-14-00153.1.

Stohl, A., S. Eckhardt, C. Forster, P. James, N. Spichtinger, and P. Seibert, 2002: A replacement for simple back trajectory calculations in the interpretation of atmospheric trace substance measurements. *Atmos. Environ.*, **36**, 4635–4648, doi:10.1016/S1352-2310(02)00416-8.

——, C. Forster, A. Frank, P. Seibert, and G. Wotawa, 2005: Technical note: The Lagrangian particle dispersion model FLEXPART version 6.2. *Atmos. Chem. Phys.*, **5**, 2461–2474, doi:10.5194/acp-5-2461-2005.

Stunder, B. J. B., 1996: An assessment of the quality of forecast trajectories. *J. Appl. Meteor.*, **35**, 1319–1331, doi:10.1175/1520-0450(1996)035<1319:AAOTQO>2.0.CO;2.

——, J. L. Heffter, and R. R. Draxler, 2007: Airborne volcanic ash forecast area reliability. *Wea. Forecasting*, **22**, 1132–1139, doi:10.1175/WAF1042.1.

Tupper, A., J. Davey, P. Stewart, B. Stunder, R. Servranckx, and F. Prata, 2006: Aircraft encounters with volcanic clouds over Micronesia, Oceania, 2002/03. *Aust. Meteor. Mag.*, **55**, 289–299.

Wain, A. G., S. Lee, G. A. Mills, G. D. Hess, M. E. Cope, and N. Tindale, 2006: Meteorological overview and verification of HYSPLIT and AAQFS dust forecasts for the duststorm of 22-24 October 2002. *Aust. Meteor. Mag.*, **55**, 35–46.

Wang, Y., A. F. Stein, R. R. Draxler, J. D. de la Rosa, and X. Zhang, 2011: Global sand and dust storms in 2008: Observation and HYSPLIT model verification. *Atmos. Environ.*, **45**, 6368–6381, doi:10.1016/j.atmosenv.2011.08.035.

Webley, P. W., B. J. B. Stunder, and K. G. Dean, 2009: Preliminary sensitivity study of eruption source parameters for operational volcanic ash cloud transport and dispersion models—A case study of the August 1992 eruption of the Crater Peak vent, Mount Spurr, Alaska. *J. Volcanol. Geotherm. Res.*, **186**, 108–119, doi:10.1016/j.jvolgeores.2009.02.012.

Wen, D., J. C. Lin, D. B. Millet, A. Stein, and R. Draxler, 2012: A backward-time stochastic Lagrangian air quality model. *Atmos. Environ.*, **54**, 373–386, doi:10.1016/j.atmosenv.2012.02.042.

Wendell, L. L., 1972: Mesoscale wind fields and transport estimates determined from a network of wind towers. *Mon. Wea. Rev.*, **100**, 565–578, doi:10.1175/1520-0493(1972)100<0565:MWFATE>2.3.CO;2.

Witham, C. S., M. C. Hort, R. Potts, R. Servranckx, P. Husson, and F. Bonnardot, 2007: Comparison of VAAC atmospheric dispersion models using the 1 November 2004 Grimsvötn eruption. *Meteor. Appl.*, **14**, 27–38, doi:10.1002/met.3.

Yerramilli, A., and Coauthors, 2012: An integrated WRF/HYSPLIT modeling approach for the assessment of PM2.5 source regions over the Mississippi Gulf Coast region. *Air Qual. Atmos. Health*, **5**, 401–412, doi:10.1007/s11869-010-0132-1.

Zhao, C., A. E. Andrews, L. Bianco, J. Eluszkiewicz, A. Hirsch, C. MacDonald, T. Nehrkorn, and M. L. Fischer, 2009: Atmospheric inverse estimates of methane emissions from Central California. *J. Geophys. Res.*, **114**, D16302, doi:10.1029/2008JD011671.

The Life Cycles of Extratropical Cyclones

Edited by Melvyn A. Shapiro and Sigbjørn Grønås

Containing expanded versions of the invited papers presented at the International Symposium on the Life Cycles of Extratropical Cyclones, held in Bergen, Norway, 27 June–1 July 1994, this monograph will be of interest to historians of meteorology, researchers, and forecasters. The symposium coincided with the 75th anniversary of the introduction of Jack Bjerknes's frontal-cyclone model presented in his seminal article, "On the Structure of Moving Cyclones." The monograph's content ranges from a historical overview of extratropical cyclone research and forecasting from the early eighteenth century into the mid-twentieth century, to a presentations and reviews of contemporary research on the theory, observations, analysis, diagnosis, and prediction of extratropical cyclones. The material is appropriate for teaching courses in advanced undergraduate and graduate meteorology.

***The Life Cycles of Extratropical Cyclones* is available for $75 list/$55 members.**
To order, visit www.ametsoc.org/amsbookstore, or see the order form at the back of this issue.